Original Research Article

Parallel signal acquisition time with timing with dirty templates in ultrawideband systems using delay-hopping-transmitted reference receiver

Taijung Huang

Longyan University, Institute of Mathematics and Information Engineering, Longyan of Fujian Province 364012, China

Abstract: Synchronization poses a major challenge to UWB systems due to the low acquisition time in UWB. This study develops an Shared Loopded Delay -Line for FD-IR-UWB receivers to improve the synchronization performance. The proposed parallel search architecture reduces the search time of the symbol boundaries. Moreover, one branch needs a time delay element, since SDL was proposed to lower the implementation complexity of the parallel search architecture. Finally, simulations and theoretical analysis show that the proposed architecture obtains a lower MSE and a higher PD than other alternatives.

Keywords: Index Terms—frame-differential (FD); Shared looped delay-line (SLD); Acquisition timing with dirty templates (TDT)

1. Introduction

UWB radios could use frequencies in the range 3.1-10.6 GHz[1]. UWB can thus save the bandwidth, low cost, and low power consumption requirements of next-generation CE devices. Different UWB systems have been proposed, including TH-IR UWB, MB-OFDM UWB, and DS UWB. In TH-IR UWB systems^[2], data are transmitted using trains of pulses on the order of nanoseconds. TH-UWB systems achieve a fine multi-path resolution capability and low power consumption, which makes TH-IR UWB systems viable candidates suitable shortrange or indoor wireless communications^[3].

A important issue to TH-UWB systems is time synchronization since the information bearing waveforms are pulselike. Moreover, low power pulses through the multipath channel is unknown at receiver at the synchronization scheme.

Hence, peak-picking of output of a sliding correlator between the received and the transmitted template is not only optimal in dense multipath, but also leads an unacceptably slow acquisition speed^[4].

TR receivers^[5] have a important advantage for coherent receivers, in that they capture power from multipath components at a low complexity. However, the reference pulses are corrupted by noise or interference. FD receivers, unlike TR schemes, transmit data by applying DPSK at the frame-level^[6], then there is no need to TR pulses. Hence, FD receivers have a lower IFI than TR schemes, and are therefore more suitable for high data rate applications. Witrisal^[6] proposed an equivalent system for FD-IR-UWB systems, but also did not manufacture the synchronization problems.

Yang and Giannakis^[7] proposed a new synchronization criterion, termed "timing with dirty templates" (TDT). The TDT exploits the fact that the cross-correlation of these TDT exhibits a maximum at the accurate symbol time. Although TDT is blind in the situation that they do not need TH code, they are inoperable in multi-user environment in which other users adopt the same training patterns.

This study creates a synchronization algorithm for multiuser and multipath environment designated as "PS-SLD. The receiver of PS-SLD resembles that of the FD-IR-UWB system proposed by Witrisal^[6], however includes an additional SLD. Moreover, the synchronization scheme of the PS-SLD is similar to that of TDT algorithms^[7] in that the PS-SLD algorithm also determines the maximum accumulated output by testing all of the candidate offsets. However, the candidate offsets considered by TDT algorithms belong to the interval $[0, T_s]$, however those of the PS-SLD belong to the interval $[0, T_f]$, referred as the "uncertainty region", owing to its parallel search mechanism. Finally, The simulation results also confirm that PS-SLD achieves a higher PD and a lower MSE than TDT, particularly in multi-user environment.

2. Signal model

As discussed in [2], the transmitted waveform from the user k is expressed as

$$s_k = \sum_{i=-\infty}^{\infty} \sum_{j=0}^{N_f - 1} d_{k,i} w(t - iT_s - jT_f - c_{k,j} T_c),$$
(1)

where k is the user index; i is the symbol index; j is the frame index; $d_{k,i} \in \{+1,-1\}$ is the data sequence of the kth active user; w(t) is the transmitted pulse waveform; T_s is the symbol duration; T_f is the pulse repetition time; $\{c_{k,j}\}_{j=0}^{N_f-1}$ is the TH code, and T_c is the chip duration.

As discussed in [6], let be the offset between the pth and the (p+1)th transmitted pulses from the user k, where

 $Dk,p = Tf + (ck,[p+1]_{Nf} - ck,[p]_{Nf}) \times Tc$ for $p \in [0,Nf-1]$, and $[\cdot]_{Nf}$ indicates the modulo operation with base N_f . The $s_k(t)$ is given by

$$s_k(t) = \sum_{i=-\infty}^{\infty} \sum_{j=0}^{N_f - 1} d_{k,i} w(t - iT_s - c_{k,0} T_c - \sum_{p=0}^{j-1} D_{k,p}),$$
(2)

where $\sum_{n=0}^{-1} D_{k,p} = 0$ is defined.

The multipath corresponding to every user k is modeled as a tap delay line with L_k+1 taps. The amplitudes $\{\alpha_{k,l}\}_{l=0}^{L_k}$ and delays $\{\tau_{k,l}\}_{l=0}^{L_k}$ of the taps are assumed to be constant over. The channel impulse response is given by

$$h_k(t) = \sum_{l=0}^{L_k} \alpha_{k,l} \delta(t - \tau_k - \tau_{k,l}), \tag{3}$$

where $\tau_{k,}^{0}=0$ is defined, $\tau_{k} \in [0, T_{s})$ represents the propagation delay of the first arrival signal, and $\tau_{k,Lk}$ represents t delay spread. The collected waveform of all the users has the form

$$r(t) = \sum_{k=0}^{N_u - 1} s_k(t) * h_k(t) + n(t)$$

$$= \sum_{k=0}^{N_u - 1} \sum_{i=-\infty}^{\infty} \sum_{j=0}^{N_f - 1} \sum_{l=0}^{L_k} d_{k,i} \alpha_{k,l} w(t - iT_s - c_{k,0}T_c - \sum_{n=0}^{j-1} D_{k,p} - \tau_k - \tau_{k,l}) + n(t),$$

$$(4)$$

where N_u is the number of users, and n(t) denotes the AWGN. Since $\{\alpha_{k,l}\}_{l=0}^{L_k}$ and $\{\tau_{k,l}\}_{l=0}^{L_k}$ are constant over one symbol duration, let $v_{k,l}(t)$ =

$$\sum_{l=0}^{L_k} \alpha_{k,l} w(t - iT_s - c_{k,0}T_c - \sum_{p=0}^{-1} D_{k,p} - \tau_k - \tau_{k,l}) j$$

, and then

 $v_{k,i,j}(t) = v_{k,i,0}(t - \sum_{p=0}^{j-1} D_{k,p})$. Eq. (3) can therefore be recast

as

$$r(t) = \sum_{k=0}^{N_u - 1} \sum_{i=-\infty}^{\infty} \sum_{j=0}^{N_f - 1} d_{k,i} v_{k,i,0} \left(t - \sum_{p=0}^{j-1} D_{k,p}\right) + n(t).$$
 (5)

3. Parallel signal acquisition with ps-sld algorithm

As demonstrated in Fig.1, $y_{k,q}(t)$ denotes the output from the N_f branches of the SLD, where $q \in [0, N_f - 1]$ is the index of a branch, k denotes index of the desired user. The term $y_{k,q}(t)$ has the form

$$y_{k,q}(t) = \sum_{m=q}^{N_f - 1 + q} r(t - \tau) \times r(t - D_{k,[m]_{N_f}} - \tau)$$

$$*\delta(t - \sum_{p=m+1}^{N_f - 1 + q} D_{k,[p]_{N_f}}).$$
(6)

where $\tau \in [0, T_f)$ denotes the candidate offsets. Let $\tau = n \times T^{\Delta}$, where the integer $n \in [0, N_f - 1]$ is the step index, and T^{Δ} is the interval among candidate offsets.

Furthermore, $z_{k,q}[n]$ denotes the integration output of $y_{k,q}(t)$ based on every step indexes (n). $z_{k,q}[n]$ is given by

$$z_{k,q}[n] = \int_{(i+1)T_s + c_{k,q}T_c}^{(i+1)T_s + c_{k,q}T_c} y_{k,q}(t)dt$$

$$= \int_{(i+1)T_s + c_{k,q}T_c}^{(i+1)T_s + c_{k,q}T_c} \sum_{m=q}^{N_f - 1 + q} r(t - nT_{\Delta}) \times r(t - D_{k,[m]N_f} - nT_{\Delta}) * \delta(t - \sum_{p=m+1}^{N_f - 1 + q} D_{k,[p]N_f})dt,$$
(7)

where T_w indicates the integration window. Generally, $T_w \le \tau_{k,Lk}$ reasonably be assumed. Substituting Eq. (5) into Eq. (7) yields

$$z_{k,q}[n] = \sum_{m=q}^{N_f - 1 + q} \int_{(i+1)T_s + c_{k,q}T_c}^{(i+1)T_s + c_{k,q}T_c} \left\{ \sum_{k_1 = 0}^{N_u - 1} \sum_{i_1 = -\infty}^{\infty} \sum_{j_1 = 0}^{N_f - 1} d_{k_1,i_1} v_{k_1,i_1,0} (t - \sum_{p=0}^{j_1 - 1} D_{k_1,p} - nT_{\Delta}) + n(t - nT_{\Delta}) \right\}$$

$$\times \left\{ \sum_{k_2 = 0}^{N_u - 1} \sum_{i_2 = -\infty}^{\infty} \sum_{j_2 = 0}^{N_f - 1} d_{k_2,i_2} v_{k_2,i_2,0} (t - D_{k,[m]N_f}) - \sum_{p=0}^{j_1 - 1} D_{k_1,p} - nT_{\Delta} + n(t - D_{k,[m]N_f} - nT_{\Delta}) \right\}$$

$$*\delta(t - \sum_{n=m+1}^{N_f - 1 + q} D_{k,[p]N_f}) dt.$$

$$(8)$$

Because the desired user index is k, and the desired output is the multiplication of the mth and the (m+1)th

pulses of the *i*-th or the (i+1)th symbols following the delay element, $D_{k, m}^{[\]} f$, the desired terms can be extracted with indexes $k^1 = k^2 = k$,

$$i=i+\lfloor (m+1)/N \rfloor, i=i+\lfloor m/N \rfloor, j=m+1, \text{ and } j=1$$
 f 2 f 1 2 m from Eq. (8). Accordingly, $z_{k,q}[n]$ is given by

$$\begin{split} z_{k,q}[n] &= \sum_{m=q}^{N_f-1+q} \int_{(i+1)T_s+c_{k,q}T_c}^{(i+1)T_s+c_{k,q}T_c} \left\{ d_{k,i+\lfloor (m+1)/N_f \rfloor} \times \\ v_{k,i,0}(t-\sum_{p=0}^m D_{k,[p]N_f} - nT_\Delta) \times d_{k,i+\lfloor m/N_f \rfloor} \times \\ v_{k,i,0}(t-D_{k,[m]N_f} - \sum_{p=0}^{m-1} D_{k,[p]N_f} - nT_\Delta) \right\} \\ &\times \delta(t-\sum_{p=m+1}^{N_f-1+q} D_{k,[p]N_f}) dt + \Psi[n] \\ &= \sum_{m=q}^{N_f-1+q} (d_{k,i+\lfloor (m+1)/N_f \rfloor} \times d_{k,i+\lfloor m/N_f \rfloor}) \times \\ \int_{(i+1)T_s+c_{k,q}T_c}^{(i+1)T_s+c_{k,q}T_c+T_w} v_{k,i,0}^2(t-\sum_{p=0}^m D_{k,[p]N_f}) \\ &-nT_\Delta) * \delta(t-\sum_{p=m+1}^{N_f-1+q} D_{k,[p]N_f}) dt + \Psi[n] \\ &= \sum_{m=q}^{N_f-1+q} (d_{k,i+\lfloor (m+1)/N_f \rfloor} \times d_{k,i+\lfloor m/N_f \rfloor}) \times \\ \int_{(i+1)T_s+c_{k,q}T_c}^{(i+1)T_s+c_{k,q}T_c} v_{k,i,0}^2(t-\sum_{p=0}^{N_f-1+q} D_{k,[p]N_f}) \\ &-nT_\Delta) dt + \Psi[n] \\ &= (N_f-1+d_{k,i}d_{k,i+1}) \int_{(i+1)T_s+c_{k,q}T_c}^{(i+1)T_s+c_{k,q}T_c} v_{k,i,0}^2(t-T_s-\sum_{p=0}^{q-1} D_{k,p}-nT_\Delta) dt + \Psi[n], \end{split}$$
 (9)

where $\Psi[n]$ denotes the noise and interference terms. -

Eq. (9) more produces

$$\begin{split} z_{k,q}[n] &= (N_f - 1 + d_{k,i}d_{k,i+1}) \int_{(i+1)T_s + c_{k,q}T_c + T_w}^{(i+1)T_s + c_{k,q}T_c + T_w} \\ & \left\{ \sum_{l=0}^{L_k} \alpha_{k,l} w(t - T_s - \sum_{p=0}^{q-1} D_{k,p} - nT_\Delta - iT_s - c_{k,0}T_c - \tau_k - \tau_{k,l}) \right\}^2 dt + \Psi[n]. \end{split}$$
 Since $\sum_{p=0}^{q-1} D_{k,p} + c_{k,0}T_c = qT_f + c_{k,q}T_c$, $z_{k,q}[n]$ is given by

$$z_{k,q}[n] = (N_f - 1 + d_{k,i}d_{k,i+1}) \int_{(i+1)T_s + c_{k,q}T_c + T_w}^{(i+1)T_s + c_{k,q}T_c} \left\{ \sum_{l=0}^{L_k} \alpha_{k,l} w(t - (i+1)T_s - nT_\Delta - qT_f - c_{k,q}T_c - \tau_k - \tau_{k,l}) \right\}^2 dt + \Psi[n]$$

$$= (N_f - 1 + d_{k,i}d_{k,i+1}) \int_0^{T_w} \left\{ \sum_{l=1}^{L_k} \alpha_{k,l} w(t - nT_\Delta - qT_f - \tau_k - \tau_{k,l}) \right\}^2 dt + \Psi[n].$$

Assuming that ${\tau_{k,l}}^1-{\tau_{k,l}}^2\geq T_p$ where $l_1\neq l_2$, then $w(t-\frac{\tau_{k,l_1}}{T_w})$ and $w(t-\tau_{k,l_2})$ are uncorrelated. In this case,

$$\int_0^{\infty} \frac{(-\Delta - qT_f - \tau_k - \tau_{k,l_1}) \times w(t - nT_\Delta - qT_f - \tau_k - t_k, l_1^2)}{dt} = 0$$
 for each $l_1 \neq l_2$.

Finally, $z_{k,q}[n]$ is given by

$$z_{k,q}[n] = (N_f - 1 + d_{k,i}d_{k,i+1}) \sum_{l=1}^{L_k} \alpha_{k,l}^2 \int_0^{T_w} w^2(t - \tau_{k,l} - nT^{\Delta} - qT_f - \tau_k)dt + \Psi[n].$$
(10)

If $\Psi[n]$ in Eq. (10) is neglected, then $z_{k,q}[n]$ exhibits a maximum when $\tau_k = -(qT_f + nT^{\Delta})$. The estimated branch index (q) and estimated step index (n) at which $z_{k,q}[n]$ exhibits a maximum can then be determined according to the criterion

$$[n, \hat{q}] = \arg\max z_{k,q}[n], \tag{11}$$

 $q \in [0, N_i - 1], n \in [0, N_i - 1]$

where $N_i := \lceil T_f/T_\Delta \rceil$. Thus, the estimated propagation delay is given by $\tau_k^* = -(qT_f + nT_f^\Delta)$.

Since the symbol boundaries $aret_{symbol}^{(i)} = (i+1)T_s + \tau_k$, the estimated symbol boundaries can be derived by

$$t_{symbol}^{(i)} = (i+1)T_s + \tau_k = iT_s + (T_s - \hat{q}T_f - \hat{n}T_\Delta).$$
(12)

PERFORMANCE ANALYSIS

The preceding section describes how to determine the estimated symbol boundaries $\hat{t}_{symbol}^{(i)}$, as shown in Eq. (12). This section introduces the analysis of the probability of detection (PD). In Eq. (11), the estimators $q^{\hat{}}$ and $n^{\hat{}}$ aim to find the true branch index $(q^{\hat{}})$ and step index $(n^{\hat{}})$. The probability of detection is denoted as

$$P_{d}(q^{*}, n^{*}) = Pr\{\hat{q} = q^{*} \text{ and } \hat{n} = n^{*}\}$$

$$] = \arg \max = Pr\{z_{k,q^{*}}[n^{*}_{q,n} z_{k,q}[n]\}.$$
(13)

Significantly, at any given SNR, $P_d(q^*, n^*)$ generally depends on n^* . This is because the noise terms of $z_{k,q}[n]$ are correlated across n since observation windows are overlapping^[7]. For analytical tractability, rather than estimating the true symbol boundaries, this section discusses a coarse timing acquisition method. The coarse timing acquisition aims to find q^* and n^* such that $0 \le \varepsilon^{\tau} < T^{\Delta}$ is satisfied, where $\varepsilon^{\tau} := |T_s - q^*T_f - n^*T^{\Delta}|$ represents the inaccuracy between the declared symbol boundary and the true symbol boundary. Furthermore, T^{Δ} can be equal to or larger than the integration window T_w for coarse timing acquisition. In this case, independence of $T_{k,q}[n]$ can be reasonably assumed across T_s and T_s and T_s are the integration windows are non-overlapping.

The integration output based on each determined ε^{τ} is given as $z_{k,q}^{(\varepsilon_{\tau})}[n]$. For the desired user k, the probability density function (pdf) of $z_{k,q}^{(\varepsilon_{\tau})}[n]$ is denoted as $f_{q,n}(z|\varepsilon^{\tau})$. The probability of detection (PD) for every q^* and n^* based on a determined ε^{τ} is given as

$$p(q^*, n^*|\varepsilon_{\tau}) = \int_{-\infty}^{\infty} f_{q^*, n^*}(z|\varepsilon_{\tau}) \times \prod_{(q, n) \neq (q^*, n^*)} \left(\int_{-\infty}^{z} f_{q, n}(x|\varepsilon_{\tau}) dx \right) dz.$$

$$(14)$$

For each ε^{τ} , since two possible values of n^* could satisfy the inequality, $|T_s - q^*T_f - n^*T^{\Delta}| < T^{\Delta}$, the PD for coarse timing acquisition is given by

$$P_d(\varepsilon^{\mathsf{r}}) := p(q^*, n^{*1}|\varepsilon^{\mathsf{r}}) + p(q^*, n^{*2}|\varepsilon^{\mathsf{r}}), (15) \text{ where } n^{*1} \text{ and } n^{*2} \text{ satisfy } -T^{\Delta} < T_s - q^*T_f - n^{*1}T^{\Delta} \le 0, \text{ and } 0 \quad s - f - 2 \le T \quad q^*T \quad n^*T^{\Delta} < T^{\Delta}.$$
Assuming that $\varepsilon_T \le T - q^*T - 1 \le T$

is uniformly distributed over interval of $[0,T^{\Delta})$. The PD can then be obtained by averaging all possible ε^{τ} over $[0,T^{\Delta})$, and is thus given by

$$P_{d} = \frac{1}{T_{\Delta}} \int_{0}^{T_{\Delta}} P_{d}(\varepsilon_{\tau}) d\varepsilon_{\tau}$$

$$= \frac{1}{T_{\Delta}} \int_{0}^{T_{\Delta}} \left\{ p(q^{*}, n_{1}^{*} | \varepsilon_{\tau}) + p(q^{*}, n_{2}^{*} | \varepsilon_{\tau}) \right\} d\varepsilon_{\tau}.$$
(16)

Substituting Eq. (14)into Eq. (16) yields

$$P_{d} = \frac{1}{T_{\Delta}} \int_{0}^{T_{\Delta}} \left\{ \int_{-\infty}^{\infty} f_{q^{*},n_{1}^{*}}(z|\varepsilon_{\tau}) \times \prod_{(q,n)\neq(q^{*},n_{1}^{*})} \int_{-\infty}^{z} f_{q,n}(x|\varepsilon_{\tau}) dx dz \right\} + \left\{ \int_{-\infty}^{\infty} f_{q^{*},n_{2}^{*}}(z|\varepsilon_{\tau}) \times \prod_{(q,n)\neq(q^{*},n_{2}^{*})} \int_{-\infty}^{z} f_{q,n}(x|\varepsilon_{\tau}) dx dz \right\} d\varepsilon_{\tau}.$$

$$(17)$$

As presented in^[8], here we can also derive a lower bound from Eq. (17). It is given as

$$P_{d} \geq \underline{P_{d}} := \frac{1}{T_{\Delta}} \int_{0}^{T_{\Delta}} \left\{ \prod_{(q,n)\neq(q^{*},n_{1}^{*})} \int_{-\infty}^{\infty} f_{q^{*},n_{1}^{*}}(z|\varepsilon_{\tau}) \right.$$

$$\times \int_{-\infty}^{z} f_{q,n}(x|\varepsilon_{\tau}) dx dz \right\}$$

$$+ \left\{ \prod_{(q,n)\neq(q^{*},n_{2}^{*})} \int_{-\infty}^{\infty} f_{q^{*},n_{2}^{*}}(z|\varepsilon_{\tau}) \right.$$

$$\times \int_{-\infty}^{z} f_{q,n}(x|\varepsilon_{\tau}) dx dz \right\} d\varepsilon_{\tau}.$$

$$(18)$$

Through the central limit theorem, $z_{k,q}^{(\varepsilon_{\tau})}[n]$ can be treated as Gaussian distributed, in which case the lower bound in Eq.

(18) becomes

$$\underline{P_d} = \frac{1}{T_{\Delta}} \int_0^{T_{\Delta}} \prod_{(q,n) \neq (q^*,n_1^*)} Q \left(\frac{m_{q,n}(z|\varepsilon_{\tau}) - m_{q^*,n_1^*}(z|\varepsilon_{\tau})}{\sqrt{\sigma_{q,n}^2(z|\varepsilon_{\tau}) + \sigma_{q^*,n_1^*}^2(z|\varepsilon_{\tau})}} \right)$$

$$\sqrt{\sigma^2 (z|\varepsilon_{\tau}) + \sigma^2_{*} (z|\tau)}$$
(19)

where $Q(\bullet)$ indicates the complementary cumulative distribution function (cdf) of a standard Gaussian random variable with zero mean and unit variance, $m_{q,n}(z|\epsilon^{\tau})$ denotes the mean of $z_{k,q}^{(\epsilon_{\tau})}[n]$, and $\sigma_{q,n}^{2}(z|\epsilon^{\tau})$ denotes the variance of

$$z_{k,q}^{(\varepsilon_{\tau})}[n].$$

4. Simulations

The performance of the proposed PS-SLD algorithm was evaluated through a series of simulations. The multipath channels were generated using the UWB channel model proposed by IEEE 802.15.3a [9] with parameters of $(1/\Lambda, 1/\lambda, \Gamma, \gamma)$ =(42.9, 0.4, 7.1, 4.3) nanosecond (ns). The channel impulse response was assumed over one symbol duration. Furthermore, for each user k, an assumption was made that the propagation delay of the first arrival signal, τ_k , was uniformly distributed over the interval $[0, T_s)$ ns, where $T_s = N_f \times T_f$. The frame duration was specified as T_f =35 ns, and each symbol comprised of N_f =32 frames. The desired user (indexed as k) was assigned a TH code{ $c_{k,j}$ } $_{j=0}^{N_f-1}$ that satisfied $D_{k,p} \neq D_{k,q}$ for every $p \neq q$. The remaining users were assigned random TH codes uniformly distributed over the interval $[0, N_c \times T_c)$ with N_c =35 and T_c =1 ns. The training sequence for the data-aided (DA) TDT was composed of a repeated pattern (1, 1, -1, -1) for users, but the transmitted datum, $d_{k,p}$ is randomly generated in the PS-SLD algorithm. The integration window, T_w , was specified as 35ns in all of the PS-SLD simulations. Finally, in all simulations, when comparing PS-SLD with TDT algorithms, T^{Δ} was defined to equal T_i in $T^{(7)}$.

Figure 2 illustrates the PD for PS-SLD algorithm obtained using computer simulation and Monte Carlo simulation. Simulation results of the PS-SLD algorithm are similar to the Monte Carlo simulation results of Eq. (17), indicating that Eq. (17) forms sound theoretical values of PD. Moreover, the Monte Carlo simulation results also demonstrate that Eq. (18) and Eq. (19) are identical.

Figure 3 shows the comparison of PD of the PS-SLD algorithm and the TDT algorithms. Simulation results indicate that the PS-SLD algorithm obtains a higher PD than its TDT counterparts. This result is reasonable, since the SLD receiver utilizes the unique time interval between two successive pulses, i.e. $D_{k,p}$, as the time delay when correlating the received signal with the time-delayed signal. Hence, the SLD receiver is more robust to noise and interference than the dirty templates receiver.

Although the TDT algorithms are blind, the PD of TDT algorithm is only around $1/N_u$, because the receiver can't determine the desired user's signals from other users' signals in a multi-user environment. In this case, the performance of PS-SLD is better than that of TDT algorithms in a multi-user environments.

 $+\prod_{\varepsilon}Q\Big({}^{m_{q,n}(z|\varepsilon_{\tau})-m_{q^*,n_2^*}(z|\varepsilon_{\tau})}\Big)d\varepsilon_{\tau}, \ T_{\Delta}=T_c$ **Figures 4** and **5** compare the MSE between PS-SLD and TDT algorithms for different T^{Δ} , indicating that TDT algorithms with $T^{\Delta}=T_f$ perform nearly the same as that with , but the performance of MSE for the PS-SLD with performs superior to that with $T^{\Delta}=T_f$. Notably, the PD of TDT algorithms is lower than that of the PS-SLD algorithm in **Figure 3**, but the normalized MSE of TDT algorithms is not higher than that of the PS-SLD algorithm in **Figure 4**, because the constant of the estimated symbol boundaries for PS-SLD algorithm is larger than that for TDT algorithms while $T^{\Delta}=T_f$. Although the performance in MSE of PS-SLD is a little larger than that of TDT algorithms while $T^{\Delta}=T_f$, the PS-SLD algorithm performs superior to that of TDT algorithms when $T^{\Delta}=T_c$.

5. Conclusions

This investigation proposes an effective non-data aided (NDA) timing synchronization scheme PS-SLD. Although PS-SLD has a higher hardware complexity than TDT schemes, its uncertain region is bounded within one frame duration, and is only $1/N_f$ of that of the TDT algorithms. Simulation results indicate that the PS-SLD algorithm obtains a higher PD and a lower normalized MSE than the TDT algorithms in both multipath and multi-user environments.

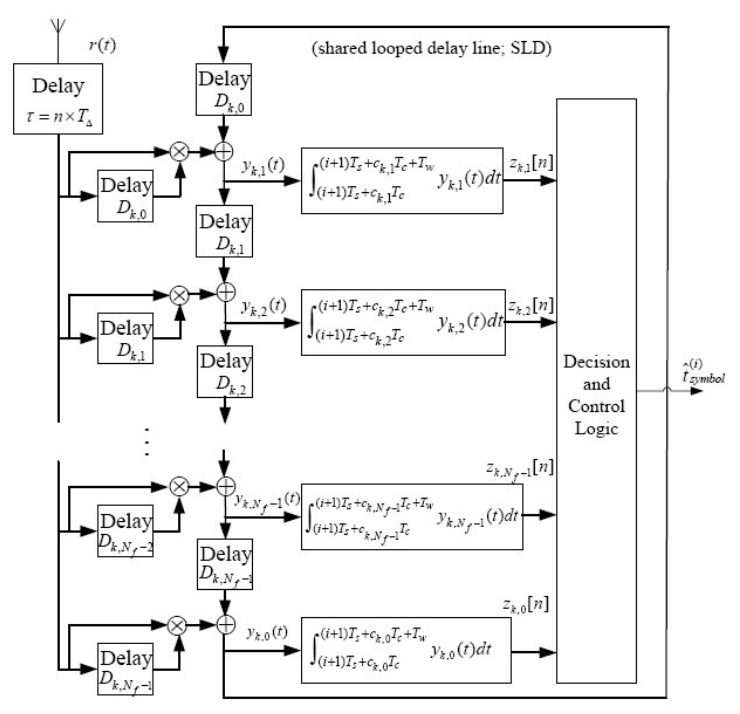


Figure 1. Block diagram of shared looped delay-line (SLD) receiver for the kth user.

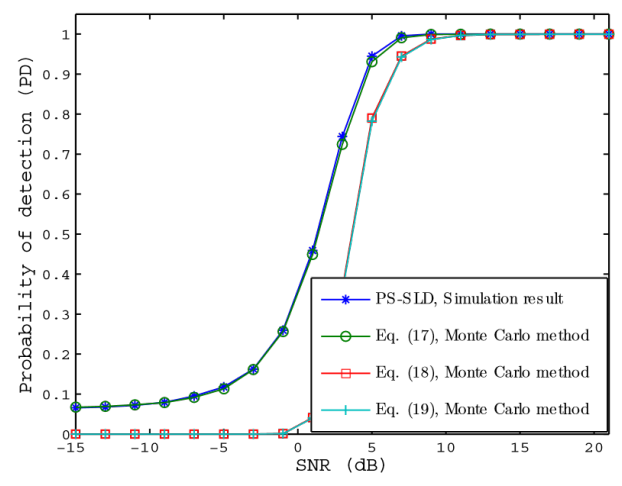


Figure 2. PD simulations and theory results, with $T\Delta$ =Tf in a single-use link.

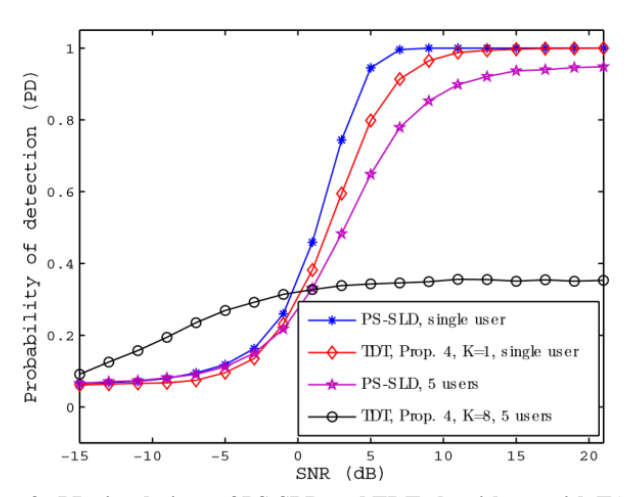


Figure 3. PD simulations of PS-SLD and TDT algorithms, with $T\Delta$ =Tf.

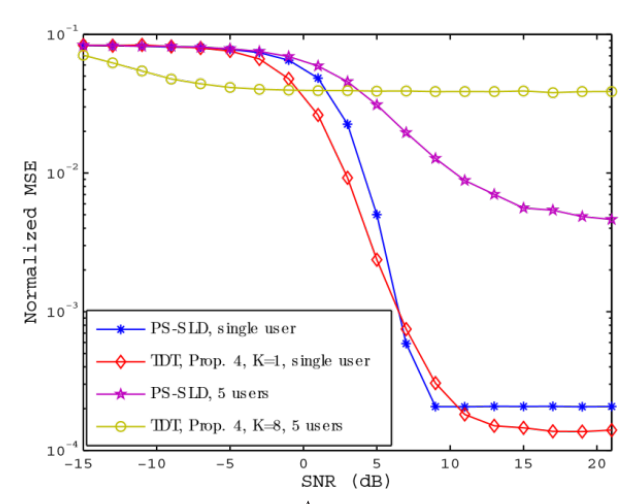


Figure 4. Normalized MSE with $T^{\Delta}=T_{c}$ (normalized with respect to T_{s}^{2}).

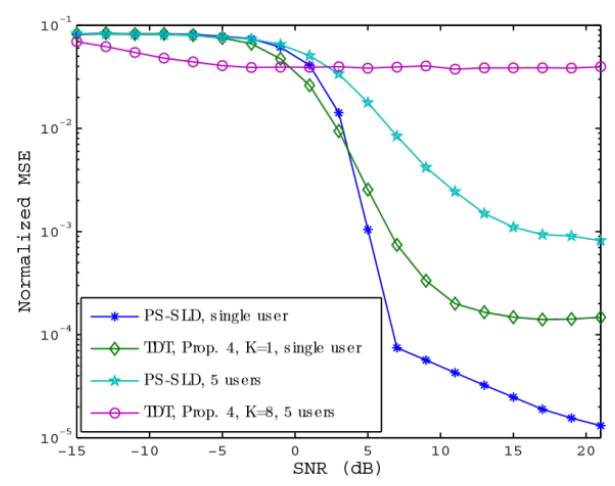


Figure 5. Normalized MSE with $T^{\Delta}=Tc$. (normalized with respect to T_s^2).

References

- [1] FCC First Report and Order: In the matter of revision of part 15 of the commission's rules regarding ultra-wideband transmission systems, FCC 02-48, Apr. 2002.
- [2] M. Z. Win and R. A. Scholtz, "Ultra-wide Bandwidth Time-hopping Spread-spectrum Impulse for

- Wireless Multiple-access Communications," IEEE Transactions on Communications, vol. 48, pp. 679-689, Apr. 2000.
- [3] M. Z. Win, R. A. Scholtz, and M. A. Barnes, "Ultra-wide Bandwidth Signal Propagation for Indoor Wireless Communications," Proceedings of the IEEE Internal Conf. on Communications, vol. 1, June 1997, pp. 56-60.
- [4] L. Yang and G. B. Giannakis, "Low-Complexity Training for Rapid Timing Acquisition in Ultra-Wideband Communications," in Proceedings of IEEE Global Telecommunications Conference, San Francisco, CA, December 1-5, 2003, vol. 2, pp. 769-773.
- [5] Tony Q. S. Quek and Moe Z. Win, "Analysis of UWB TransmittedReference Communication Systems in Dense Multipath Channels," IEEE J. Select. Areas Commun., vol. 23, no 9, pp. 1863-1874, Sept. 2005.
- [6] K. Witrisal, G. Leus, M. Pausini and C. Krall, "Equivalent System Model and Equalization of Differential Impulse Radio UWB Systems," IEEE J. Sel. Areas Commun., vol. 23, no. 9, pp. 1851-1862, Sept. 2005.
- [7] L. Yang and G. B. Giannakis, "Timing Ultra-wideband Signals with Dirty Templates," IEEE Trans. Commun., vol, 53, no. 11, pp. 1952 1963, Nov. 2005.
- [8] L. W. Hughes, "A Simple Upper Bound on the Error Probability for Orthogonal Signals in White Noise," IEEE Trans. Commun., vol. 40, no. 4, p. 670, Apr. 1992.
- [9] D. B. Maria-Gabriella and G. Guerino, Understanding Ultra Wide Band Radio Fundamentals, 1st ed., Prentice Hall. Jun. 17, 2004, pp. 277 294.